



Published in final edited form as:

Invest Radiol. 2022 January 01; 57(1): 13–22. doi:10.1097/RLI.0000000000000808.

Coronary Artery Calcium Scoring *Toward a New Standard*

Gijs D. van Praagh, MSc^{*,†}, Jia Wang, PhD[‡], Niels R. van der Werf, MSc^{§,||}, Marcel J.W. Greuter, PhD^{†,¶}, Domenico Mastrodicasa, MD^{*,#}, Koen Nieman, MD, PhD^{#,**}, Robbert W. van Hamersvelt, MD, PhD[§], Luuk J. Oostveen, BSc^{††}, Frank de Lange, PhD^{††}, Riemer H.J.A. Slart, MD, PhD^{†,‡,‡}, Tim Leiner, MD, PhD[§], Dominik Fleischmann, MD^{*,#}, Martin J. Willemink, MD, PhD^{*}

^{*}Department of Radiology, Stanford University School of Medicine, Stanford, CA

[†]Medical Imaging Center, University of Groningen, University Medical Center Groningen, Groningen, the Netherlands

[‡]Department of Environmental Health and Safety, Stanford University, Stanford CA

[§]Department of Radiology, University Medical Center Utrecht, Utrecht

^{||}Department of Radiology and Nuclear Medicine, Erasmus Medical Center, Rotterdam

[¶]Department of Robotics and Mechatronics, University of Twente, Enschede, the Netherlands

[#]Department of Cardiovascular Institute

^{**}Department of Cardiology, Stanford University School of Medicine, Stanford, CA

^{††}Department of Medical Imaging, Radboud University Medical Center, Nijmegen

^{‡‡}Department of Biomedical Photonic Imaging, University of Twente, Enschede, the Netherlands.

Abstract

Objectives: Although the Agatston score is a commonly used quantification method, rescan reproducibility is suboptimal, and different CT scanners result in different scores. In 2007, McCollough et al (*Radiology* 2007;243:527–538) proposed a standard for coronary artery calcium quantification. Advancements in CT technology over the last decade, however, allow for improved acquisition and reconstruction methods. This study aims to investigate the feasibility of a reproducible reduced dose alternative of the standardized approach for coronary artery calcium quantification on state-of-the-art CT systems from 4 major vendors.

Materials and Methods: An anthropomorphic phantom containing 9 calcifications and 2 extension rings were used. Images were acquired with 4 state-of-the-art CT systems using routine protocols and a variety of tube voltages (80–120 kV), tube currents (100% to 25% dose levels), slice thicknesses (3/2.5 and 1/1.25 mm), and reconstruction techniques (filtered back projection and iterative reconstruction). Every protocol was scanned 5 times after repositioning the phantom to assess reproducibility. Calcifications were quantified as Agatston scores.

Correspondence to: Gijs D van Praagh, MSc, Medical Imaging Center, Department of Nuclear Medicine and Molecular Imaging, University Medical Center Groningen, Hanzeplein 1, 9713 GZ, Groningen, the Netherlands. g.d.van.praagh@umcg.nl

Supplemental digital contents are available for this article. Direct URL citations appear in the printed text and are provided in the HTML and PDF versions of this article on the journal's Web site (www.investigativeradiology.com).

Results: Reducing tube voltage to 100 kV, dose to 75%, and slice thickness to 1 or 1.25 mm combined with higher iterative reconstruction levels resulted in an on average 36% lower intrascanner variability (interquartile range) compared with the standard 120 kV protocol. Interscanner variability per phantom size decreased by 34% on average. With the standard protocol, on average, 6.2 ± 0.4 calcifications were detected, whereas 7.0 ± 0.4 were detected with the proposed protocol. Pairwise comparisons of Agatston scores between scanners within the same phantom size demonstrated 3 significantly different comparisons at the standard protocol ($P < 0.05$), whereas no significantly different comparisons arose at the proposed protocol ($P > 0.05$).

Conclusions: state-of-the-art CT systems of 4 different vendors, a 25% reduced dose, thin-slice calcium scoring protocol led to improved intrascanner and interscanner reproducibility and increased detectability of small and low-density calcifications in this phantom. The protocol should be extensively validated before clinical use, but it could potentially improve clinical interscanner/interinstitutional reproducibility and enable more consistent risk assessment and treatment strategies.

Keywords

coronary artery calcium; computed tomography; Agatston score; phantom study; CT protocol

Quantification of coronary artery calcifications (CACs) with the Agatston score using cardiac CT is a strong predictive marker for future cardiovascular events in asymptomatic individuals at low-to-intermediate risk.^{1,2} Although CT technology has improved tremendously over the last decade, the CAC quantification standard—using 120 kV, 3 or 2.5 mm slices, and filtered back projection (FBP)—has not been renewed since its introduction in 2007 by McCollough et al.³ Larger CT detector coverage, more efficient detector technology, higher spatial resolution, shorter gantry rotation time, increased x-ray tube power, and improved reconstruction algorithms are nowadays available to reduce the image noise of cardiac CT and thus allow for radiation dose reduction.⁴ A large body of evidence has shown that the reproducibility of currently used CAC acquisition and quantification methods is limited as it can result in reclassifications.⁴⁻⁷ Hence, the current quantification standard for CAC scoring should be updated.

Rutten et al⁸ demonstrated in patients that small variations of scan starting position affect the reproducibility of Agatston scores with a potential risk of reclassification in 9% of the individuals. In addition, Willeminck et al⁵ found a substantial intervender variability of the Agatston score, which resulted in a modest cardiovascular risk reclassification in up to 6.5% of ex vivo hearts. Coronary artery calcium reproducibility can be improved by reducing slice thickness and tube voltage.^{4,5,9} The current, standard slice thickness of 3 or 2.5 mm results in a suboptimal spatial resolution and a possible underestimation of small or less dense calcifications due to partial volume effects. The use of thinner slices reduces these effects, improves reproducibility, and enhances detectability of (micro)calcifications, where 1 microcalcification is typically 0.5 to 15 μm .^{4,9,10} This may be an opportunity for risk factor modification and thus prevention of cardiovascular events, as nonzero CAC scores are associated with higher risk for future events, whereas zero scores are strong negative predictors.^{4,9-11} Reducing tube voltage results in 2 effects: it will reduce radiation dose when other settings remain unchanged; concurrently, it will increase CT attenuation, which

can potentially improve the detectability and quantification of less dense calcifications. Iterative reconstruction (IR) can be used to reduce radiation dose without compromising image noise compared with routine dose FBP.^{12,13} Multiple studies have shown that radiation dose reduction over 50% is possible in CAC imaging with IR.¹² Modifying the CAC acquisition method will result in more accurate estimation of coronary calcified lesions as well as reduced radiation, hence important for consistent risk assessment and treatment.

This study aims to investigate the feasibility and reproducibility of a reduced dose alternative of the standardized approach for CAC quantification on state-of-the-art CT systems from 4 major vendors.

MATERIALS AND METHODS

Phantom

For all experiments, a commercially available static anthropomorphic thoracic phantom (Thorax; QRM, Möhrendorf, Germany) was used. At the position of the heart, a cardiac calcification insert (CCI; QRM, Möhrendorf, Germany) was placed, containing 9 small cylindrical calcifications with different sizes and densities (diameters: 1, 3, and 5 mm; densities: 200, 400, and 800 mg/cm³ calcium hydroxyapatite [CaHA]), and 2 large calibration rods (one water equivalent and one 200 mg/cm³ CaHA). The thoracic phantom simulates a small-sized patient (anterior-posterior × lateral, 200 × 300 mm). Two additional tissue-equivalent oval rings (extension rings; QRM, Möhrendorf, Germany) were used to simulate medium- and large-sized patients (250 × 350 mm and 300 × 400 mm, respectively; Fig. 1).

Image Acquisition and Reconstruction

All phantom sizes were scanned using state-of-the-art CT systems from 4 different vendors (scanner A: SOMATOM Force, Siemens Healthineers, Erlangen, Germany; scanner B: Revolution, GE Healthcare, Milwaukee, WI; scanner C: iCT, Philips Healthcare, Best, the Netherlands; scanner D: Aquilion One PRISM Edition, Canon Medical Systems, Otawara, Japan). Acquisition and reconstruction parameters are listed in Tables 1 and 2. A reference tube voltage of 120 kV and a decreased tube voltage of 100 kV were used. An exploratory scan session on each CT system showed that tube power limitations arose for 80 kV; therefore, 100 kV was the most optimal reduced tube potential for all 4 vendors (Supplementary Table 1, <http://links.lww.com/RLI/A641>). Tube current was modulated with anatomic based automatic exposure control on scanners A, B, and D. For scanner C, this was not available. Volumetric CT dose indices (CTDI_{vol}) were kept similar between CT systems. Reference dose levels (100%) were chosen as CTDI_{vol} values of 1.5, 3.3, and 7.0 mGy for small, medium, and large phantom size, respectively, which is in line with clinically used protocols.^{15–17} The following parameters were varied on the scanners: radiation dose, slice thickness, and IR level (Table 2). Radiation dose was incrementally reduced by lowering CTDI_{vol}, resulting in 4 dose levels: 100%, 75%, 50%, and 25%. Multiple reconstructions were made per scan with varying slice thickness and increment: 3.0 and 1.0 mm on scanners A, C, and D, and 2.5 and 1.25 mm on scanner B. Besides FBP, 3 settings of IR algorithms were used on every scanner. Every protocol was scanned 5 times with small repositioning

(approximately 5 mm translational and 2 degrees rotational) of the phantom after each scan to measure and correct for interscan variability.¹⁸

Quantification of Coronary Calcifications

The calcifications inside the phantom were quantified as Agatston scores using the validated fully automated quantification method (FQM).¹⁹ The standard 130 Hounsfield unit (HU) threshold was used for 120 kV scans. Due to increased x-ray beam attenuation, the threshold was increased to 147 HU for 100 kV scans as proposed by Nakazato et al.,²⁰ and effects in similar Agatston results with decreased tube voltage, decreased slice thickness, and use of IR shown by Hou et al.²¹ In addition, the output of FQM gave the following information about each individual calcification: volume, mass, maximum area, and mean Agatston weight factor (based on maximum HU value per area).²² Volume was quantified according to Callister et al.²³ Volume, area, and weight factor were only used for clarification purposes of the changes in Agatston scores due to acquisition or reconstruction adjustments.

Image Noise

The output of FQM included the number of detectable calcifications and noise level. Noise level was defined as the standard deviation of pixel values in HU within a circular region of interest of 1.5 cm² placed in the center slice of the water equivalent rod. McCollough et al.³ described a noise target measured in the water equivalent rod of 20 HU for small- and medium-sized phantoms and 23 HU for the large-sized phantom. Noise levels below these targets were not selected to keep radiation dose levels reasonable, thus not too high. After review of the experimental data, we chose an upper threshold as well of 30 HU for the small- and medium-sized phantom and 35 HU for the large-sized phantom to keep image noise reasonable and reduce the possibility of false-positives.

Statistical Analysis

The interquartile range (IQR) of the total Agatston scores from all phantom sizes and all CT systems scanned with the standard protocol were used as a reference range for total Agatston scores to keep scores similar to the current protocol. We compared the different scan protocols based on intrascanner and interscanner reproducibility, calcification detectability, and image noise as described previously. On that basis, a protocol for each scanner was proposed and compared with the currently used standard protocol. Intrascanner reproducibility was defined as the calcium score IQR of the 5 repetitions within that protocol. Interscanner reproducibility was defined as IQR of the sum of all calcium scores from that protocol acquired on all 4 CT systems. Change of variability was thus calculated as: $(-1 + IQR_{new\ protocol}/IQR_{current\ protocol}) \times 100\%$. The FQM used a mask based on the physical locations of all calcifications in the phantom. A calcification was defined detected when connected components above the 130 or 147 HU threshold arose within the mask. To show trends, results in the text are shown in median (IQR) for all phantom sizes and scanners combined unless indicated otherwise. More detailed comparisons between scores are displayed in the figures. Only pairwise comparisons were done for the total Agatston scores of the standard and proposed protocol. After testing for normality, differences were evaluated with Friedman tests and post hoc Dunn tests with Bonferroni correction. *P*

values less than 0.05 were considered statistically significant. SPSS version 25 (IBM Corp, Armonk, NY) was used for statistical analyses.

RESULTS

Intrascanner Reproducibility

Agatston score variability of repeated acquisitions on the same scanner slightly increased after decreasing the tube potential (see Fig. 2 and Supplementary Figures 1 and 2, <http://links.lww.com/RLI/A641>), that is, IQR of 100 kV, 100% dose, thick slices, and routine reconstruction protocol changed with 7% (–26% to 140%). Reducing slice thickness in addition to the decreased tube potential lowered intrascanner variability with IQR changes of –54% (–76% to –44%). Comparing this 100 kV, thin slice, 100% dose protocol with tube current reductions to 75%, 50%, and 25% resulted in Agatston score IQR changes of 22% (–39% to 141%), 0 (–45% to 86%), and 99% (40% to 519%), respectively. Similar trends were seen in volume scores (see Supplementary Results, <http://links.lww.com/RLI/A641>).

Calcification Detectability

Table 3 shows the number of detected calcifications per protocol and phantom size of all scanners combined. Of the 9 calcification inserts, the number of detected calcifications with the standard protocol was on average 6.2 ± 0.4 . This was similar with standard slice thickness, 100 kV, 100% dose, and routine reconstruction. Additional reduction of the slice thickness increased the number of detected calcifications with on average 1 calcification. Protocols with 100 kV, thin sections, routine reconstruction, and reduced radiation dose resulted in a similar number of detected calcifications. Increasing IR levels showed a trend toward a slight decrease in detected number of calcifications. The higher number of calcifications detected was due to small calcifications of 800 or 400 mg/cm³ CaHA.

Radiation Dose and Image Noise

Noise levels differed between scanners, but noise levels of the standard protocols were equal or below the lower noise limit on all scanners (see Fig. 3 and Supplementary Figures 3 and 4, <http://links.lww.com/RLI/A641>). Thin-sliced protocols at 100 kV with 50% or 25% dose resulted in noise levels exceeding the upper threshold on scanner C, even with highest IR level for medium- and large-sized phantoms, respectively. Thin-sliced protocols with 75% dose stayed within the noise thresholds when intermediate or high IR was used for all scanners, except scanner C. Noise levels exceeded the upper threshold at scanner C when 100 kV, 75% dose, thin slices, and intermediate IR was used at the medium- and large-sized phantom, respectively.

Proposed Protocol

Based on the above results, we proposed the following protocols: for scanners A and B: 100 kV, 75% dose, thin slices, intermediate IR; for scanners C and D: 100 kV, 75% dose, thin slices, high IR (Table 4). Figure 4 shows axial images of the phantom obtained with the standard and proposed protocol on all scanners.

Compared with the standard protocol, these protocols resulted in an improved intrascanner variability (IQR) of -12% , -68% , and -73% for scanners A, B, and C, respectively, and a slight increase of 8% for scanner D. Also, improved intrascanner volume variability was found for all scanners and improved mass-variability for scanners C and D (see Supplementary Results, <http://links.lww.com/RLI/A641>).

With these proposed protocols, interscanner variability changed with -55% , -35% , and -13% for small-, medium-, and large-sized phantoms, respectively. Interscanner variability improved for all volumes and mass scores as well, except for the mass scores in the large-sized phantom (see Supplementary Results, <http://links.lww.com/RLI/A641>).

Pairwise comparisons of Agatston scores between scanners within the same phantom size showed that the standard protocol resulted in significantly different scores between scanners: scanner B versus C for the small phantom (558 [556–574] vs 702 [661–730], $P < 0.01$), scanner B versus C for the large phantom (588 [567–603] vs 653 [635–685], $P = 0.02$), and scanner B versus D for the small phantom (558 [556–574] vs 720 [703–733], $P = 0.02$). All other comparisons were not significantly different ($P > 0.05$). In contrast, Agatston scores were not significantly different between scanners when using the proposed new protocols ($P > 0.05$).

Noise levels for small-, medium-, and large-sized phantoms with the proposed protocols ranged from 23.7 (23.3–24.2) to 27.9 (27.5–29.3) for scanner A, 26.1 (26.0–27.1) to 29.1 (28.3–29.4) for scanner B, 21.3 (21.1–21.6) to 35.1 (33.5–36.9) for scanner C, and 20.8 (20.4–22.4) to 23.3 (21.9–24.5) for scanner D.

The number of detectable calcifications with the proposed protocols was 7.1 ± 0.2 , 7.1 ± 0.4 , and 7.0 ± 0.5 for the small-, medium-, and large-sized phantoms, respectively.

Per-Calcification Analysis

Median Agatston scores of 800 mg/cm^3 CaHA calcifications changed with the proposed protocol by -15% and -14% for the large- and medium-sized calcifications, respectively (see Fig. 5 and Supplementary Figures 5 and 6, <http://links.lww.com/RLI/A641>). Median Agatston scores slightly decreased on average for the large-sized 400 mg/cm^3 CaHA calcification (-2%), whereas scores increased for the medium-sized 400 mg/cm^3 CaHA calcification (11%). Median Agatston scores of 200 mg/cm^3 CaHA calcifications increased on average with 39% and 43% for the large- and medium-sized calcifications, respectively.

The proposed protocol resulted in calcification volumes closer to the physical volume for all calcifications (see Supplementary Results and Supplementary Fig. 7, <http://links.lww.com/RLI/A641>). Mass scores remained similar compared with the standard protocol (Supplementary Fig. 8, <http://links.lww.com/RLI/A641>). Maximum areas and weight factors remained similar or slightly increased (Supplementary Figs. 9 and 10, <http://links.lww.com/RLI/A641>). Weight factors especially increased in 200 mg/cm^3 CaHA calcifications.

Intrascanner variability of the Agatston score decreased for most calcifications. Medians of IQR changes per-calcification were -68% , 5% , and -30% for large-sized 800 , 400 , and 200

mg/cm³ CaHA calcifications, and -81%, -37%, and 39% for medium-sized 800, 400, and 200 mg/cm³ CaHA calcifications, respectively.

Furthermore, interscanner variability of Agatston scores per calcification decreased, resulting in IQR changes of -63%, -29%, and -34% for large-sized 800, 400, and 200 mg/cm³ CaHA calcifications, and -60%, -44%, and -8% for medium-sized 800, 400, and 200 mg/cm³ CaHA calcifications, respectively (Fig. 5).

DISCUSSION

Our multivendor phantom study showed that an updated reduced dose, thin-slice CT acquisition protocol for CAC scoring resulted in improved intrascanner and interscanner variability and detectability of small- and low-density calcifications. The proposed protocol decreased volume variability of calcifications and thus decreased influence of the partial volume effect, resulting in volumes closer to their physical volume. Also, 1 additional small calcification was detected, and an increase in area and weight factor, especially for low-density calcifications, showed improved visibility. We aimed to update the 2007 CAC quantification standard by evaluating multiple protocols with the same phantom setup. For 4 state-of-the-art CT systems, we established an updated CAC quantification protocol by combining lower tube voltage (100 kV), reduced radiation dose (CTDI_{vol} 1.1, 2.5, and 5.3 mGy for small-, medium-, and large-sized patients, respectively), thinner slices (1- or 1.25-mm), and higher IR levels (ADMIRE 3, ASiR-V 50%, iDose⁴ 5, or AIDR 3D strong).

Multiple important factors call for an update of the current standard.^{4,11} First, in the last decade, CT technology has remarkably improved.⁴ Second, recent research from Blaha et al²⁴ has shown that the shape and distribution of CAC are important contributors to cardiovascular risk stratification. Third, Criqui et al²⁵ found an inversely proportional association between CAC density and future cardiovascular events, therefore making it important to accurately quantify low-density calcifications. Fourth, there is a substantial intrascanner and interscanner variability with the current CAC quantification protocols, possibly causing different treatment approaches for the same patient on different scanners or in different hospitals.^{5,8} Last, Han et al²⁶ recently demonstrated that a small but nonnegligible number of patients with zero CAC score actually did have CACs, missed by the current protocol. The presence of these plaques was associated with higher risk for major adverse cardiovascular events.

Multiple phantom and patient studies have been conducted to evaluate radiation dose reduction for CAC CT scans by lowering kV and/or mAs with or without IR.^{12,15,27-29} Also, multiple studies evaluated the effect of slice thickness on CAC scores.^{9,18,30-33} No studies have tested a variation of all 4 parameters (tube voltage, tube current, slice thickness, and reconstruction technique) on current state-of-the-art CT systems of multiple vendors. Vonder et al³⁴ varied tube voltages, dose levels, and ADMIRE levels with a dedicated phantom containing 100 small calcifications on a single CT system with conventional 3-mm slice thickness. They found possible dose reductions of up to 60.6% with 100 kV and IR-1. The lower tube current and IR level compared with our study can be explained by the 3-mm slices, as thinner slices result in more noise. Groen et al³⁵ varied tube voltage and slice

thickness on 1 CT scanner with the same phantom. They found an optimal protocol of 100 kV and 3-mm slices that resulted in similar Agatston scores and CAC detectability compared with traditional electron beam tomography, thus, not intending to improve detectability or reproducibility.

Mantini et al³⁰ showed in patients that thinner slice reconstructions led to significant upward risk reclassifications due to higher CAC scores. Two possible explanations were given (1) increased detection efficiency of small calcifications and (2) increased noise-level resulting in more false-positives. Our results support the first explanation. Although the excess risk of nonzero CAC scores by microcalcifications is not yet precisely known, the study of Hanet al²⁶ suggests that these calcifications missed by the current protocol should not be neglected.^{36,37} We expect that the updated protocol may result in improved identification of these false zero scores as detection of smaller calcifications and low-density calcifications is expected to improve. This is confirmed by our study since on average we found 1 additional small calcification with the proposed protocol compared with the current protocol. The most effective way to assess how this would translate to the clinic would be a study where patients are scanned with both the current protocol and the proposed protocol. Furthermore, we showed that IR minimizes increased noise levels of thinner sections.

A large body of evidence shows that it is safe to implement reduced radiation dose by lower tube potential and/or current, and increased IR levels.^{12,28,38} Also, the positive effects of thinner slices in CAC acquisition has been thoroughly investigated and coincide with our findings: decreased influence of the partial volume effect, improved reproducibility of CAC scores, and increased detectability of small calcifications.^{9,24,30–33} However, the effect of combining all 4 parameters in scanning patients should be further investigated.

Earlier studies have used the increased threshold before or a similar threshold, which resulted in comparable Agatston scores between the current 120 kVp protocol and a 100 kVp, lower dose protocol with 3-mm slice thickness,^{20,30,33} or with 0.5-mm slice thickness and IR.²¹ Therefore, we decided to use the same threshold and also found similar Agatston scores to the current protocol.

The supplementary section provides more specific results of volume, mass, area, and weight factor per calcification. Similar results between volumes and Agatston scores were seen, indicating that the decreased intrascanner variability is due to the decreased partial volume effects. Also, volumes of all calcifications came closer to the physical volume with the proposed protocol compared with the current standard protocol, thus resulting in a more accurate representation of the calcifications. Besides that, an increase in area and weight factor is seen in especially low-density calcifications, resulting in a maximum area closer to the physical area for small calcifications and indicating better detectability of these calcifications. This is likely due to the decreased tube voltage, hence increased attenuation.

Our study has limitations. A static phantom was used; hence, the effect of motion was not addressed. Cardiac motion can cause artifacts, which have a nonnegligible effect on CAC scores. Van der Werf et al⁴¹ showed in a dynamic phantom that heart rates have a substantial effect on Agatston and mass scores. Future research should investigate the

magnitude of this potential problem with our proposed protocol. Also, the CCI only contains 9 calcifications of 3 different sizes and densities. To investigate the exact improved detectability of our protocol, another dedicated phantom with more calcifications should be used. Although we expect the reclassification rates to be lower with the updated protocol, clinical studies should be performed to investigate whether reclassifications still occur due to the proposed protocol. Last, this protocol should be tested with new emerging techniques such as dedicated kV-independent kernels.⁴²

In conclusion, current CT acquisition protocols for CAC quantification may be updated to a protocol with 100 kV, 75% radiation dose, 1- or 1.25-mm slice thickness, and higher IR levels. On state-of-the-art CT systems of 4 different vendors, this protocol led to improved intrascanner and interscanner reproducibility and increased detectability of small and low-density calcifications. It is important to emphasize that before clinical use, the viability of this protocol should be validated in dynamic phantom and clinical studies. However, due to the improved reproducibility of the Agatston score with this protocol, this could potentially improve clinical interscanner/interinstitutional reproducibility, which would result in more consistent risk assessment and treatment strategies, and it may potentially facilitate in better risk stratification and an improved scoring method.

Supplementary Material

Refer to Web version on PubMed Central for supplementary material.

Conflicts of interest and sources of funding:

G.D.v.P. was supported in part by an unconditional grant from PUSH: a collaboration between Siemens Healthineers and the University Medical Center Groningen; the sponsor had no role in the conceptualization, interpretation of findings, writing, or publication of the article. D.M. has no activities related to the present article; he is a shareholder of and a consultant for Segmed, Inc. K.N. received institutional research support from Siemens Healthineers, Bayer Healthcare, GE Healthcare, and HeartFlow Inc. L.J.O.'s institution received a grant from Canon Medical Systems to hire a doctoral candidate to investigate subtraction CT and disclosed no other relevant relationships. D.F. has no activities related to the present article; he received research support from Siemens Healthineers and GE Healthcare, is on the speakers' bureau at Siemens Healthineers, and has ownership interest in iSchemaView; he disclosed no other relevant relationships. M.J.W. has no activities related to the present article and received a research grant from Philips Healthcare; he is a cofounder, advisor, and stockholder of Segmed, Inc; he disclosed no other relevant relationships. J.W., N.R.v.d.W., M.J.W.G., R.W.v.H., F.d.L., R.H.J.A.S., and T.L. have nothing to disclose.

REFERENCES

1. Divakaran S, Cheezum MK, Hulten EA, et al. Use of cardiac CT and calcium scoring for detecting coronary plaque: implications on prognosis and patient management. *Br J Radiol*. 2015;88:20140594. doi:10.1259/bjr.20140594.
2. Hecht H, Blaha MJ, Berman DS, et al. Clinical indications for coronary artery calcium scoring in asymptomatic patients: expert consensus statement from the Society of Cardiovascular Computed Tomography. *J Cardiovasc Comput Tomogr*. 2017;11:157–168. doi:10.1016/j.jcct.2017.02.010. [PubMed: 28283309]
3. McCollough CH, Ulzheimer S, Halliburton SS, et al. Coronary artery calcium: a multi-institutional, multimanufacturer international standard for quantification at cardiac CT. *Radiology*. 2007;243:527–538. doi:10.1148/radiol.2432050808. [PubMed: 17456875]
4. Willeminck MJ, van der Werf NR, Nieman K, et al. Coronary artery calcium: a technical argument for a new scoring method. *J Cardiovasc Comput Tomogr*. 2019;13:347–352. doi:10.1016/j.jcct.2018.10.014. [PubMed: 30366859]

5. Willemink MJ, Vliegenthart R, Takx RA, et al. Coronary artery calcification scoring with state-of-the-art CT scanners from different vendors has substantial effect on risk classification. *Radiology*. 2014;273:695–702. doi:10.1148/radiol.14140066. [PubMed: 25153157]
6. Greuter MJ, Groen JM, Nicolai LJ, et al. A model for quantitative correction of coronary calcium scores on multidetector, dual source, and electron beam computed tomography for influences of linear motion, calcification density, and temporal resolution: a cardiac phantom study. *Med Phys*. 2009;36:5079–5088. doi: 10.1118/1.3213536. [PubMed: 19994518]
7. Ulzheimer S, Kalender WA. Assessment of calcium scoring performance in cardiac computed tomography. *Eur Radiol*. 2003;13:484–497. doi:10.1007/s00330-002-1746-y. [PubMed: 12594550]
8. Rutten A, Isgum I, Prokop M. Coronary calcification: effect of small variation of scan starting position on Agatston, volume, and mass scores. *Radiology*. 2008; 246:90–98. doi:10.1148/radiol.2461070006. [PubMed: 18024437]
9. Aslam A, Khokhar US, Chaudhry A, et al. Assessment of isotropic calcium using 0.5-mm reconstructions from 320-row CT data sets identifies more patients with non-zero Agatston score and more subclinical atherosclerosis than standard 3.0-mm coronary artery calcium scan and CT angiography. *J Cardiovasc Comput Tomogr*. 2014;8:58–66. doi:10.1016/j.jcct.2013.12.007. [PubMed: 24582044]
10. Otsuka F, Sakakura K, Yahagi K, et al. Has our understanding of calcification in human coronary atherosclerosis progressed? *Arterioscler Thromb Vasc Biol*. 2014;34:724–736. doi:10.1161/ATVBAHA.113.302642. [PubMed: 24558104]
11. Blaha MJ, Mortensen MB, Kianoush S, et al. Coronary artery calcium scoring: is it time for a change in methodology? *JACC Cardiovasc Imaging*. 2017;10: 923–937. doi:10.1016/j.jcmg.2017.05.007. [PubMed: 28797416]
12. Vonder M, van der Werf NR, Leiner T, et al. The impact of dose reduction on the quantification of coronary artery calcifications and risk categorization: a systematic review. *J Cardiovasc Comput Tomogr*. 2018;12:352–363. doi:10.1016/j.jcct.2018.06.001. [PubMed: 29960743]
13. Leng S, Hruska CB, McCollough CH. Use of ionizing radiation in screening examinations for coronary artery calcium and cancers of the lung, colon, and breast. *Semin Roentgenol*. 2015;50:148–160. doi:10.1053/j.ro.2014.10.012. [PubMed: 25770345]
14. QRM Quality Assurance in Radiology and Medicine GmbH. Cardiac Calcification Insert (CCI). Published 2008. <https://www.qrm.de/content/products/anthropomorphic/cci.htm>. Accessed October 23, 2020.
15. Vingiani V, Abadia AF, Schoepf UJ, et al. Individualized coronary calcium scoring at any tube voltage using a kV-independent reconstruction algorithm. *Eur Radiol*. 2020;30:5834–5840. doi:10.1007/s00330-020-06951-1. [PubMed: 32468107]
16. Tesche C, De Cecco CN, Vliegenthart R, et al. Accuracy and radiation dose reduction using low-voltage computed tomography coronary artery calcium scoring with tin filtration. *Am J Cardiol*. 2017;119:675–680. doi:10.1016/j.amjcard.2016.10.051. [PubMed: 27986261]
17. Hecht HS, De Siqueira ME, Cham M, et al. Low- vs. standard-dose coronary artery calcium scanning. *Eur Heart J Cardiovasc Imaging*. 2015;16:358–363. doi: 10.1093/ehjci/jeu218. [PubMed: 25381303]
18. Groen JM, Greuter MJ, Vliegenthart R, et al. Calcium scoring using 64-slice MDCT, dual source CT and EBT: a comparative phantom study. *Int J Cardiovasc Imaging*. 2008;24:547–556. doi:10.1007/s10554-007-9282-0. [PubMed: 18038190]
19. van Praagh GD, van der Werf NR, Wang J, et al. Fully automated quantification method (FQM) of coronary calcium in an anthropomorphic phantom. *Med Phys*. 2021. doi:10.1002/mp.14912.
20. Nakazato R, Dey D, Gutstein A, et al. Coronary artery calcium scoring using a reduced tube voltage and radiation dose protocol with dual-source computed tomography. *J Cardiovasc Comput Tomogr*. 2009;3:394–400. doi:10.1016/J.JCCT.2009.10.002. [PubMed: 20083060]
21. Hou KY, Tsujioka K, Yang CC. Optimization of HU threshold for coronary artery calcium scans reconstructed at 0.5-mm slice thickness using iterative reconstruction. *J Appl Clin Med Phys*. 2020;21:111–120. doi:10.1002/acm2.12806. [PubMed: 31889419]

22. Agatston AS, Janowitz WR, Hildner FJ, et al. Quantification of coronary artery calcium using ultrafast computed tomography. *J Am Coll Cardiol.* 1990;15:827–832. doi:10.1016/0735-1097(90)90282-T. [PubMed: 2407762]
23. Callister TQ, Cooil B, Raya SP, et al. Coronary artery disease: improved reproducibility of calcium scoring with an electron-beam CT volumetric method. *Radiology.* 1998;208:807–814. doi:10.1148/radiology.208.3.9722864. [PubMed: 9722864]
24. Blaha MJ, Budoff MJ, Tota-Maharaj R, et al. Improving the CAC score by addition of regional measures of calcium distribution: multi-ethnic study of atherosclerosis. *JACC Cardiovasc Imaging.* 2016;9:1407–1416. doi:10.1016/j.jcmg.2016.03.001. [PubMed: 27085449]
25. Criqui MH, Denenberg JO, Ix JH, et al. Calcium density of coronary artery plaque and risk of incident cardiovascular events. *JAMA.* 2014;311:271–278. doi:10.1001/jama.2013.282535. [PubMed: 24247483]
26. Han D, Klein E, Friedman J, et al. Prognostic significance of subtle coronary calcification in patients with zero coronary artery calcium score: from the CONFIRM registry. *Atherosclerosis.* 2020;309:33–38. doi:10.1016/j.atherosclerosis.2020.07.011. [PubMed: 32862086]
27. Choi AD, Leifer ES, Yu JH, et al. Reduced radiation dose with model based iterative reconstruction coronary artery calcium scoring. *Eur J Radiol.* 2019;111:1–5. doi:10.1016/j.ejrad.2018.12.010. [PubMed: 30691659]
28. Caruso D, De Santis D, Biondi T, et al. Half-dose coronary artery calcium scoring: impact of iterative reconstruction. *J Thorac Imaging.* 2019;34:18–25. doi:10.1097/RTI.0000000000000340. [PubMed: 30036296]
29. Blobel J, Mews J, Schuijff JD, et al. Determining the radiation dose reduction potential for coronary calcium scanning with computed tomography: an anthropomorphic phantom study comparing filtered backprojection and the adaptive iterative dose reduction algorithm for image reconstruction. *Invest Radiol.* 2013; 48:857–862. doi:10.1097/RLI.0b013e31829e3932. [PubMed: 23917328]
30. Mantini C, Maffei E, Toia P, et al. Influence of image reconstruction parameters on cardiovascular risk reclassification by computed tomography coronary artery calcium score. *Eur J Radiol.* 2018;101:1–7. doi:10.1016/j.ejrad.2018.01.005. [PubMed: 29571781]
31. Horiguchi J, Matsuura N, Yamamoto H, et al. Variability of repeated coronary artery calcium measurements by 1.25-mm- and 2.5-mm-thickness images on prospective electrocardiograph-triggered 64-slice CT. *Eur Radiol.* 2008;18:209–216. doi:10.1007/s00330-007-0734-7. [PubMed: 17674003]
32. Mühlenbruch G, Thomas C, Wildberger JE, et al. Effect of varying slice thickness on coronary calcium scoring with multislice computed tomography in vitro and in vivo. *Invest Radiol.* 2005;40:695–699. doi:10.1097/01.rli.0000179523.07907.a6. [PubMed: 16230901]
33. Vliegenthart R, Song B, Hofman A, et al. Coronary calcification at electron-beam CT: effect of section thickness on calcium scoring in vitro and in vivo. *Radiology.* 2003;229:520–525. doi:10.1148/radiol.2292021305. [PubMed: 14500853]
34. Vonder M, Pelgrim GJ, Meyer M, et al. Dose reduction techniques in coronary calcium scoring: the effect of iterative reconstruction combined with low tube voltage on calcium scores in a thoracic phantom. *Eur J Radiol.* 2017;93:229–235. doi:10.1016/j.ejrad.2017.06.001. [PubMed: 28668419]
35. Groen JM, Kofoed KF, Zacho M, et al. Calcium score of small coronary calcifications on multidetector computed tomography: results from a static phantom study. *Eur J Radiol.* 2013;82:e58–e63. doi:10.1016/j.ejrad.2012.09.018. [PubMed: 23092538]
36. Blaha M, Budoff MJ, Shaw LJ, et al. Absence of coronary artery calcification and all-cause mortality. *JACC Cardiovasc Imaging.* 2009;2:692–700. doi:10.1016/j.jcmg.2009.03.009. [PubMed: 19520338]
37. Sarwar A, Shaw LJ, Shapiro MD, et al. Diagnostic and prognostic value of absence of coronary artery calcification. *JACC Cardiovasc Imaging.* 2009;2:675–688. doi:10.1016/j.jcmg.2008.12.031. [PubMed: 19520336]
38. Willeminck MJ, Takx RA, De Jong PA, et al. The impact of CT radiation dose reduction and iterative reconstruction algorithms from four different vendors on coronary calcium scoring. *Eur Radiol.* 2014;24:2201–2212. doi:10.1007/s00330-014-3217-7. [PubMed: 24889996]

39. Marwan M, Mettin C, Pflederer T, et al. Very low-dose coronary artery calcium scanning with high-pitch spiral acquisition mode: comparison between 120-kV and 100-kV tube voltage protocols. *J Cardiovasc Comput Tomogr.* 2013;7:32–38. doi:10.1016/j.jcct.2012.11.004. [PubMed: 23333186]
40. Gräni C, Vontobel J, Benz DC, et al. Ultra-low-dose coronary artery calcium scoring using novel scoring thresholds for low tube voltage protocols—a pilot study. *Eur Heart J Cardiovasc Imaging.* 2018;19:1362–1371. doi:10.1093/ehjci/jey019. [PubMed: 29432592]
41. van der Werf NR, Willemink MJ, Willems TP, et al. Influence of heart rate on coronary calcium scores: a multi-manufacturer phantom study. *Int J Cardiovasc Imaging.* 2018;34:959–966. doi:10.1007/s10554-017-1293-x. [PubMed: 29285727]
42. Tao S, Sheedy E, Bruesewitz M, et al. Technical note: kV-independent coronary calcium scoring: a phantom evaluation of score accuracy and potential radiation dose reduction. *Med Phys.* 2021;48:1307–1314. doi:10.1002/mp.14663. [PubMed: 33332626]

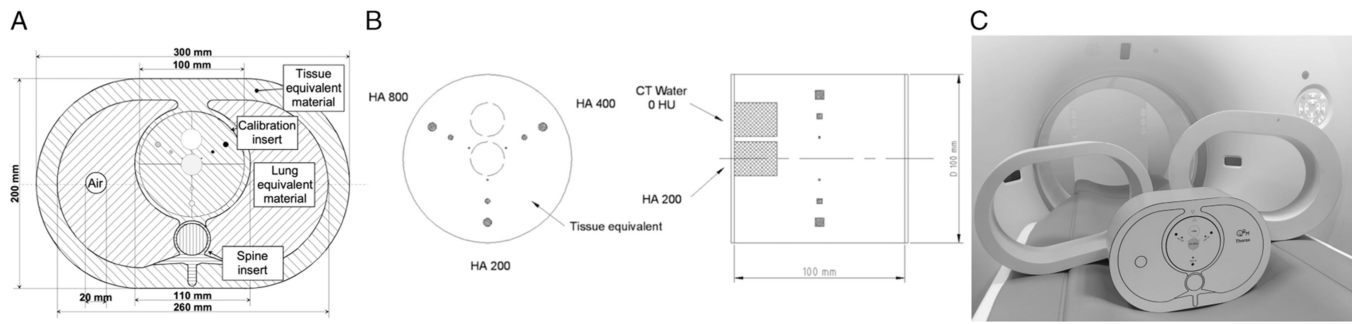


FIGURE 1.

A, Axial sketch of the thoracic phantom including the cardiac calcification insert; B, Axial and lateral sketch of the cardiac calcification insert containing the 9 calcifications and the 2 calibration rods¹⁴; C, Photo of the anthropomorphic phantom (small-sized; center) and the 2 additional rings to simulate medium-sized (left) and large-sized (right) patients. CaHA, calcium hydroxyapatite.

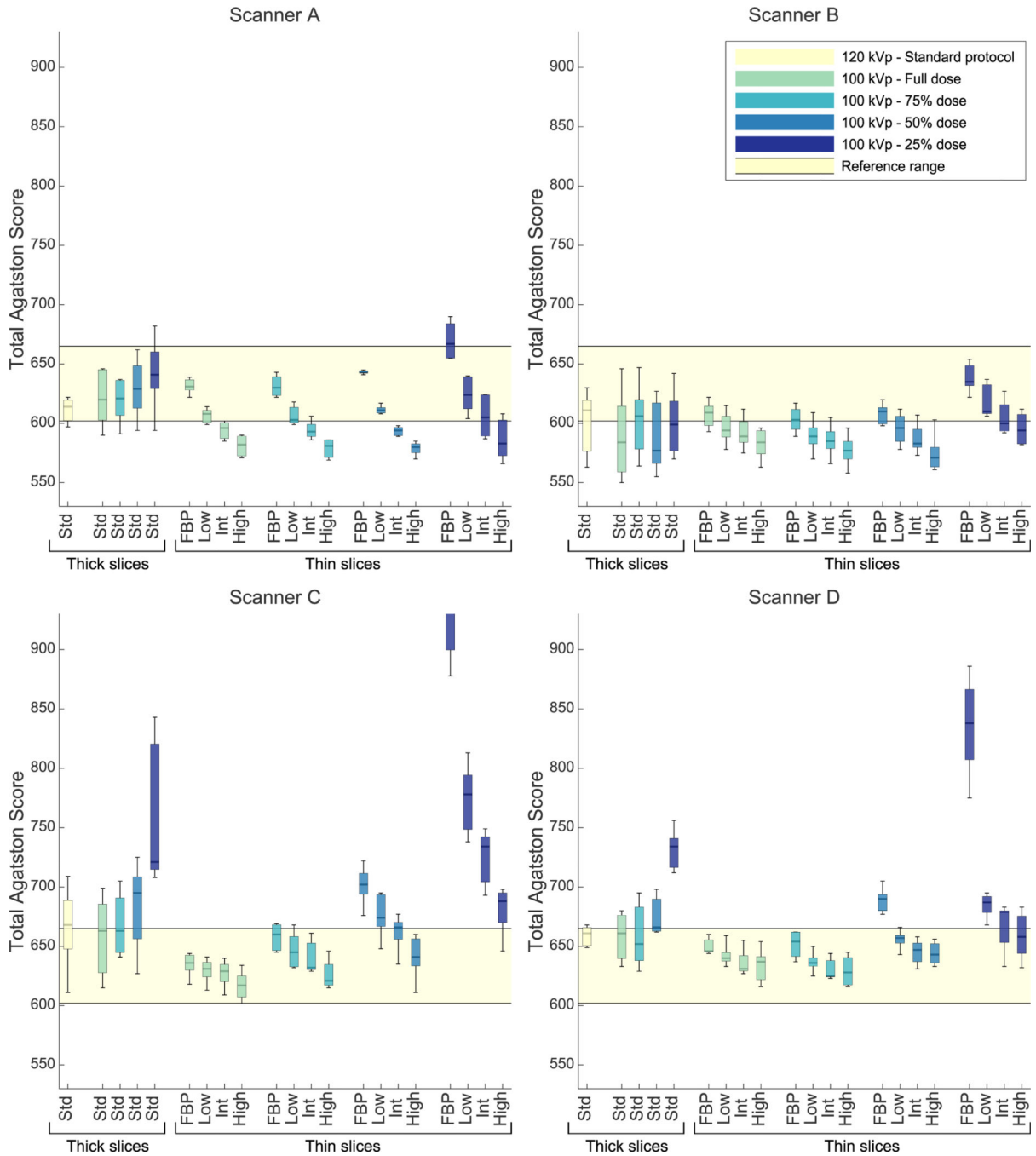


FIGURE 2. Total Agatston scores of all scanners and protocols scanned with the medium phantom. Reconstruction technique/IR levels and slice thicknesses are given on the x-axis (thick = 3 or 2.5 mm; thin = 1 or 1.25 mm). Results are grouped in dose levels. The light-yellow range is the reference range, which is the IQR of all Agatston scores from all scanners and all phantom sizes scanned with the standard protocol. Routine reconstruction (used at thick slices) for scanner A is corresponding to low IR level; for scanner B corresponding to intermediate IR level; for scanner C and D corresponding to FBP. HU thresholds were 130

HU for 120 kV scans and 147 HU for 100 kV scans. Std, standard/routine reconstruction setting; IR, iterative reconstruction; IQR, interquartile range; FBP, filtered back projection; HU, Hounsfield units. Scanner A: SOMATOM Force, Siemens Healthineers; Scanner B: Revolution, GE Healthcare; Scanner C: iCT, Philips Healthcare; Scanner D: Aquilion One PRISM Edition, Canon Medical Systems.

Author Manuscript

Author Manuscript

Author Manuscript

Author Manuscript

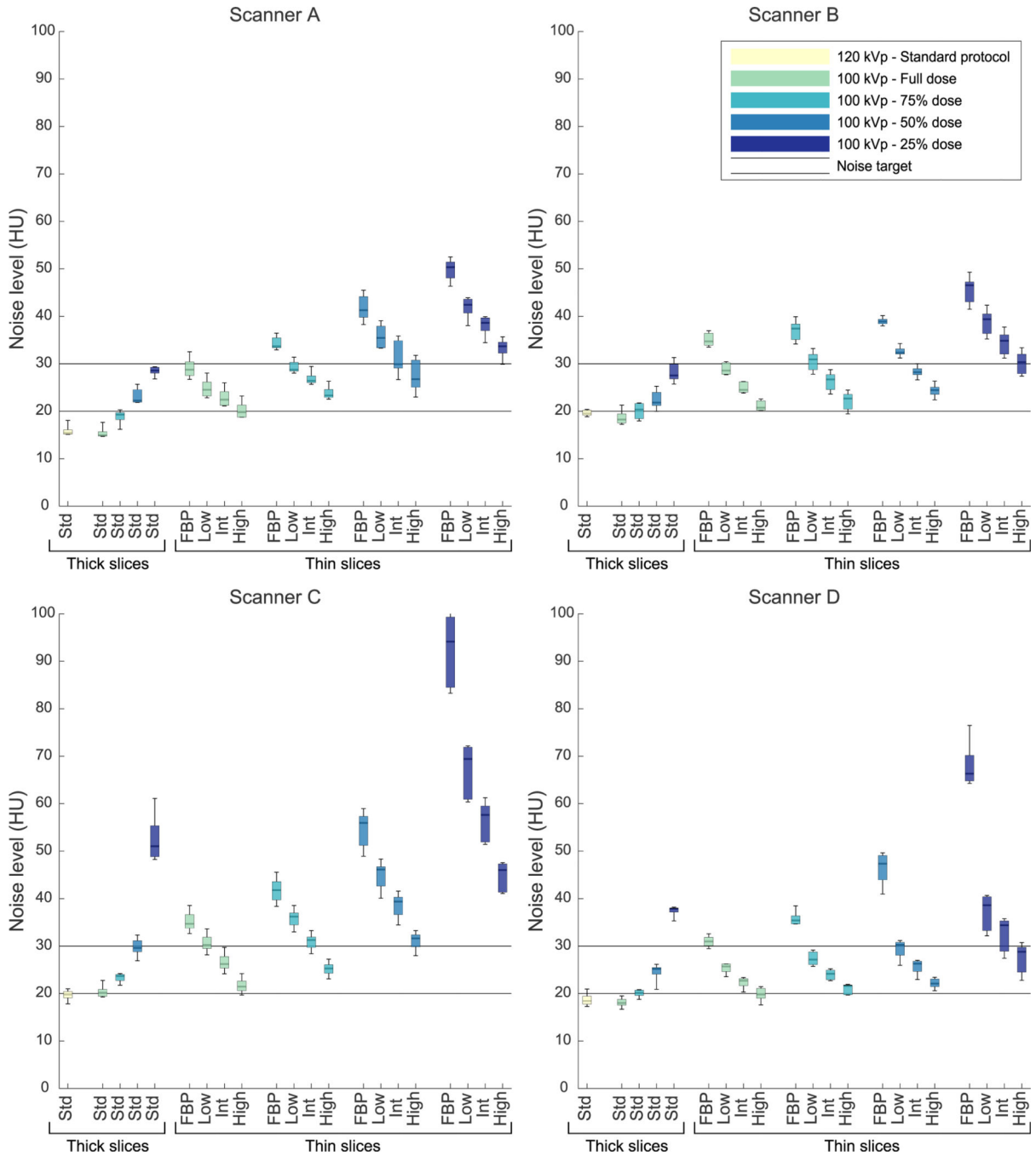


FIGURE 3. Noise levels of all scanners and protocols scanned with the medium phantom. IR levels and slice thicknesses are given on the x-axis (thick = 3 or 2.5 mm; thin = 1 or 1.25 mm). Results are grouped in dose levels. Noise levels are calculated in a circular ROI of 1.5 cm² in the center slice of a water equivalent rod as standard deviation of CT values. The 2 continuous lines show the target range. Std, standard/routine reconstruction setting; IR, iterative reconstruction; ROI, region of interest.

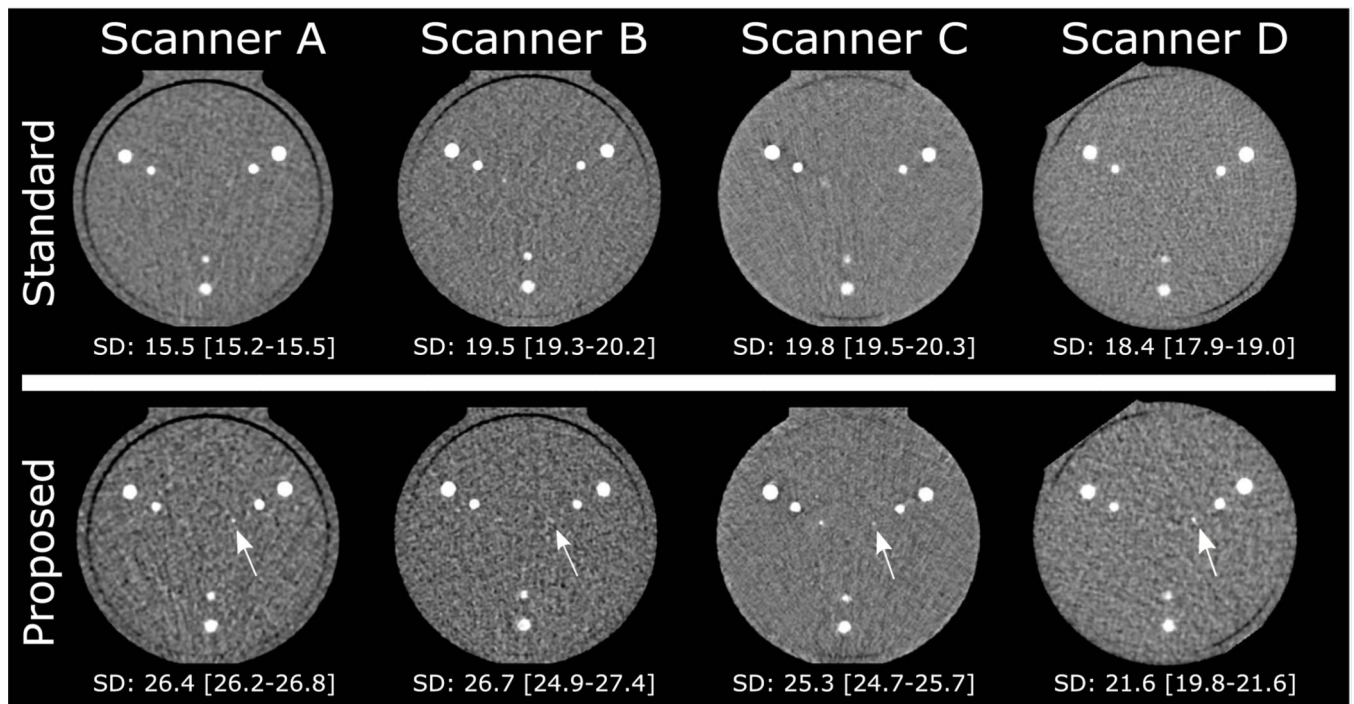


FIGURE 4.

Axial views of the center slice of the calcifications in the CCI in the medium phantom.

Upper row shows standard protocol for all scanners; lower row shows the proposed protocol for all scanners. Below every image, the median (IQR) noise level (standard deviation [SD]) of HU in the water equivalent rod is given. White arrows show the calcifications that were detected in the proposed protocol, whereas they were not detected in the standard protocol at that scanner. CCI, cardiac calcification insert; IQR, interquartile range; HU, Hounsfield units.

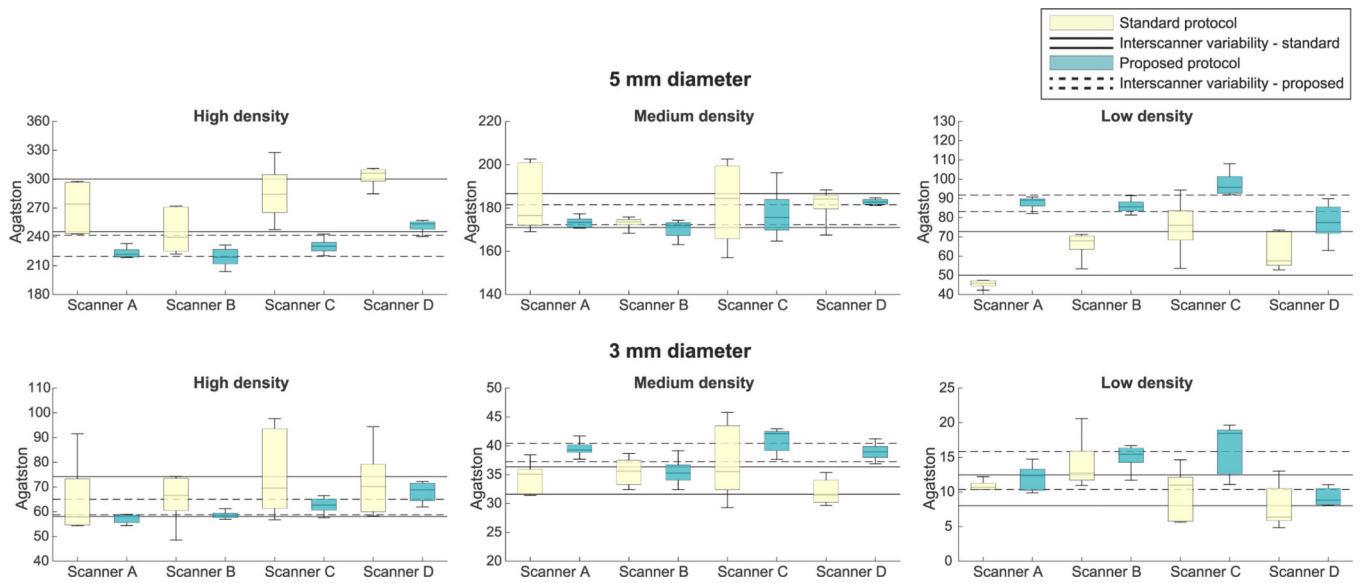


FIGURE 5. Per-calcification analysis. The Agatston scores per-calcification of the routinely used standard protocol and the proposed protocol at the medium phantom. The continuous lines show the IQR of the Agatston scores for the standard protocol. The dashed lines show the IQR of the Agatston scores for the proposed protocol. The 1 mm diameter calcifications are not shown, as they are not always detectable with every protocol. IQR, interquartile range.

TABLE 1.

Computed Tomography Acquisition and Reconstruction Parameters

| | Scanner A | | Scanner B | | Scanner C | | Scanner D | |
|-------------------------------|--------------|----------------------|------------------|-------------|--------------------------|-------------|----------------------|-------------|
| | Axial | Prospective | Axial | Prospective | Axial | Prospective | Axial | Prospective |
| Acquisition mode | | | | | | | | |
| ECG triggering | | | | | | | | |
| ECG phase (% of R-R interval) | 70% | | 75% | | 78% | | 75% | |
| Simulated heart rate, bpm | 60 | | 60 | | 60 | | 60 | |
| Rotation time, s [*] | 0.25 | | 0.28 | | 0.27 | | 0.275 | |
| Detector collimation, mm | 160 × 0.6 | | 140 × 0.625 | | 128 × 0.625 | | 200 × 0.5 | |
| Field of view, mm | 200 × 200 | | 200 × 200 | | 200 × 200 | | 200 × 200 | |
| Matrix size, pixels | 512 × 512 | | 512 × 512 | | 512 × 512 | | 512 × 512 | |
| Reconstruction kernel | Qr36d | | Standard | | XCA | | FC12 | |
| Tube current modulation | CareDose 4D | | SmartmA | | — | | Sure Exposure | |
| IR algorithms | ADMIRE (1–5) | | ASiR-V (0%–100%) | | iDose [‡] (1–7) | | AIDR 3D (mid-strong) | |
| Reconstruction settings | | Routine [‡] | | 50% | | FBP | | FBP |
| | | Low | | 30% | | 1 | | Mild |
| | | Intermediate | | 50% | | 3 | | Standard |
| | | High | | 70% | | 5 | | Strong |

^{*} Scanner B: to reach the highest possible dose with 100 kV for the large-sized phantom, the rotation time was prolonged to 0.35 seconds.

[‡] Reconstruction settings of the standard protocol were based on the institution of the CT system to simulate clinical situations.

ECG, electrocardiogram; bpm, beats per minute; IR, iterative reconstruction; FBP, filtered back projection; ADMIRE, Advanced Modeled Iterative Reconstruction (Siemens Healthineers, Erlangen, Germany); ASiR-V, Adaptive Statistical Iterative Reconstruction-V, GE Healthcare, Milwaukee, WI; iDose[‡], Philips Healthcare, Best, the Netherlands); AIDR 3D, Adaptive Iterative Dose Reduction 3D (Canon Medical Systems, Otawara, Japan).

TABLE 2.

Variable Computed Tomography Acquisition and Reconstruction Parameters

| | kV | Dose* | Slice Thickness/Increment, mm | Reconstruction Level |
|--------------------------------|-----------|--------------------------------------|--------------------------------------|----------------------------------|
| Standard protocol [†] | 120 | | 3/3 or 2.5/2.5 | Routine |
| Variable parameters | 100 | 100%, 75%, 50%, and 25% [‡] | 3/3 or 2.5/2.5 | Routine |
| | | | 1/1 or 1.25/1.25 | FBP, low, intermediate, and high |

Five repetitions were done for every protocol with small repositioning of the phantom on the table.

The standard protocol was used for every session, repetition, and phantom size.

* Full dose level (100%) is based on clinically used protocols with CTDI_{vol} value of 1.5, 3.3, and 7.0 mGy for the small, medium, and large phantom, respectively.

[†] Standard settings were based on the institution of the CT system to simulate clinical situations.

[‡] Scanner B: At the small phantom, 40% was the lowest possible dose level; at the large phantom, 89% was the highest possible dose level when prolonging rotation time to 0.35 seconds. Scanner C: At the small phantom, 33% was the lowest possible dose level.

FBP, filtered back projection.

TABLE 3.

Number of Detected Calcifications Per Protocol

| kV | Dose | Slice Thickness, mm | Reconstruction Settings | No. Calcifications | | |
|-----|------|---------------------|-------------------------|--------------------|-----------|-----------|
| | | | | Small | Medium | Large |
| 120 | 100% | 3.0/2.5 | Routine | 6.4 ± 0.5 | 6.2 ± 0.4 | 6.1 ± 0.2 |
| 100 | 100% | 3.0/2.5 | Routine | 6.2 ± 0.4 | 6.1 ± 0.3 | 6.1 ± 0.2 |
| | 75% | | | 6.1 ± 0.3 | 6.2 ± 0.4 | 6.1 ± 0.3 |
| | 50% | | | 6.1 ± 0.3 | 6.2 ± 0.4 | 6.3 ± 0.4 |
| | 25% | | | 6.3 ± 0.5 | 6.3 ± 0.5 | 6.5 ± 0.8 |
| | 100% | 1.0/1.25 | FBP | 7.4 ± 0.5 | 7.4 ± 0.5 | 7.4 ± 0.7 |
| | | | Low | 7.3 ± 0.4 | 7.2 ± 0.4 | 7.0 ± 0.6 |
| | | | Int | 7.3 ± 0.4 | 7.2 ± 0.4 | 6.9 ± 0.5 |
| | | | High | 7.1 ± 0.3 | 7.1 ± 0.3 | 6.8 ± 0.5 |
| | 75% | 1.0/1.25 | FBP | 7.6 ± 0.5 | 7.5 ± 0.6 | 7.4 ± 0.6 |
| | | | Low | 7.2 ± 0.4 | 7.4 ± 0.6 | 7.2 ± 0.6 |
| | | | Int | 7.1 ± 0.3 | 7.2 ± 0.5 | 7.0 ± 0.5 |
| | | | High | 7.1 ± 0.2 | 7.0 ± 0.2 | 6.9 ± 0.6 |
| | 50% | 1.0/1.25 | FBP | 7.5 ± 0.5 | 7.5 ± 0.6 | 7.6 ± 0.6 |
| | | | Low | 7.2 ± 0.5 | 7.2 ± 0.6 | 7.4 ± 0.6 |
| | | | Int | 7.2 ± 0.5 | 7.0 ± 0.5 | 7.3 ± 0.7 |
| | | | High | 7.0 ± 0.5 | 6.8 ± 0.4 | 6.9 ± 0.7 |
| | 25% | 1.0/1.25 | FBP | 7.5 ± 0.6 | 7.5 ± 0.8 | 7.1 ± 0.8 |
| | | | Low | 7.3 ± 0.6 | 7.1 ± 0.8 | 6.8 ± 0.8 |
| | | | Int | 6.9 ± 0.6 | 7.0 ± 0.8 | 6.8 ± 0.7 |
| | | | High | 6.8 ± 0.5 | 7.0 ± 0.8 | 6.8 ± 0.7 |

Numbers are presented in average ± standard deviation of all scanners combined.

TABLE 4.

The Proposed Acquisition and Reconstruction Protocol Per Scanner

| Scanner | kV | | CTDI _{vol} | | Slice Thickness/Increment, mm | | Iterative Reconstruction Algorithm and Level | | | |
|-------------------|--------------|--------------|---------------------|-------------|-------------------------------|------------|--|----------------|---|---|
| | All Scanners | All Scanners | A, C, and D | A, C, and D | A | B | A | B | C | D |
| Proposed protocol | 100 | 1.1/2.5/5.3* | 1/1 | 1.25/1.25 | ADMIRE.3 | ASiR-V 50% | iDose 5 | AIDR 3D strong | | |

* CTDI_{vol} values are given for small-, medium-, and large-sized patients, respectively.

CTDI_{vol}, volumetric computed tomography dose index; ADMIRE, Advanced Modeled Iterative Reconstruction; ASiR-V, Adaptive Statistical Iterative Reconstruction-V; AIDR 3D, Adaptive Iterative Dose Reduction 3D.